Seismic Response Analysis of Rocking Piers with Different Mass Ratios

Meng Jingyao
State Key Laboratory of Bridge Safety and Resilience, Beijing University of Technology, Beijing, China

Abstract: The rocking pier relaxes the constraints between the pier and the superstructure and foundation, and connects the pier and adjacent components as a whole through unbonded prestressed tendons. The rocking pier will continue to lift and close under the action of earthquake, and the rocking behavior occurs. The ratio of the mass of the superstructure to the pier usually affects the seismic response of the pier. In order to explore the influence of this factor, this paper deeply studies the seismic response of the rocking pier under different mass ratios. The research results show that the lower mass ratio will lead to the smaller inertial force at the top of the pier, so the dynamic response of the rocking pier is smaller, and the increase of the mass ratio has a limited impact on the dynamic response of the pier. At the same time, under different mass ratios, the displacement response of the damped pier may be greater than that of the undamped pier, because the damping will hinder the reset of the pier to a certain extent, resulting in an increase in the dynamic response of the pier.

Keywords: Rocking Pier; Mass Ratio; Seismic Action; Displacement Response; Viscous Damping

1. Introduction

The existing seismic design methods of building structures are mostly based on ductile design theory [1-8], which will produce serious earthquake damage such as concrete crushing and falling off in the plastic hinge area, longitudinal tendon buckling, etc., and the residual displacement is large, which is difficult to repair. The theme of the 2017 World Earthquake Engineering Congress was "Resilient Function: New Challenges in Earthquake Engineering", and the swing structure as a kind of recoverable functional structure has received extensive attention from many scholars [9]. As a kind of swing structure, the swing bridge pier weakens the constraints between the bridge pier and the adjacent components, allowing the structure to swing under the action of earthquake. Due to its special structure, the rocking bridge structure has the following typical characteristics: 1) the use of piers to swing under earthquake action to reduce the lateral stiffness, thereby prolonging the natural vibration period of the structure, thus playing a certain role in seismic isolation of the superstructure, but it is undeniable that the pier is still the main body that needs to be protected; 2) by artificially designing the deformation concentration part, the damage can be controlled at the rocking interface, and the seismic energy is consumed by additional dampers to avoid the main structure damage; 3) through the upper structure of self-weight and internal unbonded prestressed beam automatic reset, reduce the residual displacement of the structure, so as to achieve rapid repair of the bridge after the earthquake function; 4) as a kind of prefabricated structure, the components of the rocking pier can be processed in the factory, and then transported to the site for construction by prefabricated assembly, so as to achieve rapid repair of the bridge function Speed up the bridge construction process, reduce on-site construction pollution, and achieve green and low-carbon [10, 11]. Mander and Cheng [12] tested the seismic performance of rocking piers with unbonded prestressed tendons through quasi-static experiments. The results show that although the application of unbonded prestressed tendons in theoretical analysis will improve the stability, the energy dissipation capacity of the structure is obviously insufficient and needs to be improved. Cheng et al. [13] designed a rocking pier with external friction dampers and conducted a shaking table test study to evaluate the seismic performance of the pier under different parameters. Han et al. [14] studied the seismic

performance of rocking piers with external low-carbon steel bars and buckling restraint plates through quasi-static tests. At present, a certain amount of research work has been carried out on rocking piers in academic and engineering circles. However, the existing research on the structural design and seismic performance of rocking bridge piers has not yet formed a systematic and complete system of results. The wide application of rocking bridge piers in the field of engineering still needs to be carried out more in-depth and detailed research.

In this paper, firstly, the finite element model of the rocking pier is established, and the model is verified according to the test results of predecessors. The homologous seismic action is applied to the pier, and the seismic response analysis under different mass ratios is carried out. At the same time, the undamped rocking pier and the additional damped rocking pier are set up for comparative analysis. It provides a reference for the design of rocking bridge structures in the future.

2. Establishment of the Finite Element Model

2.1 Parameters of the Model

The numerical model of the rocking bridge pier constructed in this study refers to the test model of the rocking bridge pier by Guo et al. [15], which is a 1:3 scale model with actual size. Among them, the cross-section specification of the reinforced concrete pier is 350 × 350mm, and the height is 1800mm. Figure 1 The details of the reinforcement of the bridge pier, there are 16 longitudinal steel bars with a diameter of 10mm evenly distributed along the perimeter of the section. The longitudinal steel bars are only arranged inside the pier column and are not connected to the foundation part. The diameter of the transverse reinforcing bars is 6mm, and they are evenly arranged at a distance of 100mm, and the thickness of the concrete protective layer is set to 20mm. And two prestressed bars with a diameter of 16mm are selected to be built between the two holes in the center of the pier column. At the bottom of the pier, a glass fiber reinforced polymer (GFRP) protective cover with a height of 600mm and a thickness of 5mm is wrapped to protect the concrete at the bottom of the pier.

Basalt Fiber Reinforced Polymer (BFRP) bars were used to verify the prestressed steel bars, and steel strand bars were used for seismic response analysis. Among them, the elastic modulus of BFRP bars is 44GPa, and the yield strength is 1080 MPa; the elastic modulus of steel strands is 1.95×10^5MPa, the average yield strength is 1498MPa, and the prestress applied by the prestressed bars is 100kN. The upper load weight load of the pier column is 120kN. The elastic modulus of the GFRP material is 32GPa, and the ultimate strength is 558MPa. The average cubic compressive strength of the concrete used is 40.8MPa. The longitudinal reinforcement is HRB335 steel, and the yield strength is 335MPa; the transverse reinforcement is HPB300 steel, and the yield strength is 300MPa. In the follow-up seismic response analysis, the damped rocking piers and the undamped rocking piers were compared and analyzed. According to previous studies, it was found that the configuration of small damping may have adverse effects on the rocking piers, so the damping coefficient of the damped pier was set to 3N·s/mm.

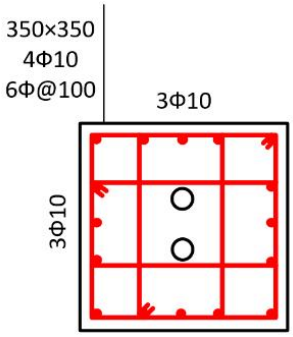

Figure 1. Rocking Pier Reinforcement Diagram

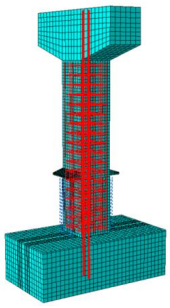

Figure 2. Finite Element Model of Rocking Piers

The finite element software ABAQUS was used to establish a refined finite element model to obtain its mechanical behavior. Figure 2 shows the finite element model of the rocking bridge pier. All concrete members were modeled using a three-dimensional eight-node reduction element (C3D8R), in which the grid size of

the column is 30mm, the foundation is 50mm, and the cover beam is 60mm. The prestressed reinforcement and GFRP sleeve were also modeled using C3D8R. The mesh size of the prestressed reinforcement is 200mm, and the sleeve is 30mm. The longitudinal and transverse reinforcement bars in the model were modeled using truss elements (T3D2).

The concrete material model uses the concrete damage plasticity (CDP) model to model all concrete members. The CDP model reflects the development of concrete cracks through material stiffness reduction, and can also achieve partial stiffness recovery under load. It can accurately simulate the performance of reinforced concrete structures under cyclic and dynamic loads [16] and is widely used in seismic analysis. Table 1-1 lists the CDP parameter value settings in ABAQUS [17, 18]. The expansion angle ψ is 30; the flow eccentricity e is 0.1; the f_{b0} is the initial biaxial compressive strength of concrete, and the f_{c0} is the initial uniaxial compressive strength of concrete. The ratio of the f_{b0}/f_{c0} is 1.16; the ratio Kc of the second stress invariant on the tensile meridian plane to the compressive meridian plane is 0.6667; the value of the viscous parameter is closely related to the calculation accuracy and convergence. The smaller the value, the more accurate the calculation result is, but the calculation speed will also be slower. If the parameter selection is reasonable, better convergence can be guaranteed. In this paper, the viscous parameter is set to 0.0005. The strength grade of concrete is 37 MPa and Poisson's ratio is 0.2.

Table 1. CDP parameters in ABAQUS

ψ	e	f_{b0}/f_{c0}	K_c	Viscous parameter
30	0.1	1.16	0.6667	0.0005

1.2 Validation of the Model

In order to verify the accuracy of the finite element model of the bridge pier, Figure 3 compares the test results of the pier with BFRP ribs with the numerical simulation results. The results show that the established finite element model is in good agreement with the force-displacement curves of the test. The lateral force when the pier and the foundation open is about 21kN, and the force-displacement relationship is basically bilinear due to the absence of additional energy-dissipating elements. The slender hysteretic curve in the test data is mainly due to the inherent friction in the structure, which is not included in the finite element model, but this does not affect the overall consistency of the two, which verifies the reliability of the finite element model.

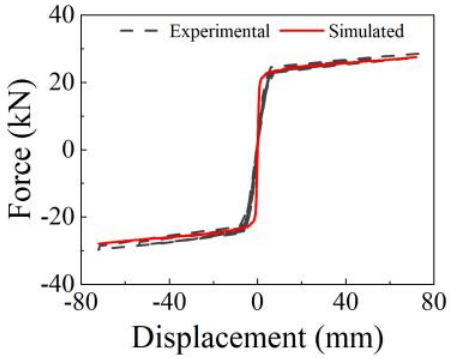

Figure 3. Model Verification of Swinging Bridge Piers

1.3 Selection of Ground Motion

Previous studies have shown that near-field ground motions have a more prominent impact on structures than far-field earthquakes, which is not conducive to the seismic safety of structural systems [19-22]. Near-field and far-field earthquakes cause huge differences in structural dynamic responses, and the fault rupture mechanism plays a key role in this phenomenon, which is an important reason for this phenomenon. In near-fault earthquakes, velocity impulses are not ubiquitous, so they can be divided into near-field pulsed and near-field non-pulsed earthquakes. This study focuses on these two types of near-field ground motions. At the same time, in order to achieve a comparative analysis, typical far-field earthquakes are also included in the research category to comprehensively consider these three types of ground motions in order to further explore their characteristics and differences. Since the test model is a 1/3 scale model, it is necessary to adopt the dimensional analysis method to obtain the similarity relationship and similarity coefficient for the finite element model, so as to reasonably scale the ground motion time. According to the capital S subscript t is equal to, the capital S subscript 1 equipment control 4 square root, medium shadow, pause, capital S subscript Rho divided, capital S subscript, capital E equipment control 4 end, square root,

the similarity coefficient of time is 0.585. In order to exclude the influence of fault mechanism, 3 different types of homologous seismic records in the Imperial Valley earthquake are selected for study. Table 2 summarizes the detailed information of the ground motion.

Table 2. Ground Motion of Different Types of Earthquakes

1979 Imperial Valley earthquake	Station	PGA	Input duration
Near-field pulse type	El Centro-7	0.5g	21.60s
Near-field pulsless type	Chihuahua	0.5g	30.17s
Far-field type	Calexico-E	0.5g	22.17s

2. Results and Discussion

2.1 Effect of Mass Ratio

In order to explore the influence of the ratio R of the mass of the superstructure to the total mass of the piers on the dynamic response of the piers, the mass ratios R were adjusted to 2, 3, 4, and 5 for analysis. Figure 4 shows the displacement responses of rocking piers with different mass ratios under near-field impulse-type earthquakes. It can be seen from the figure that when the mass ratio R=2, the overall displacement response is smaller and the duration is shorter, and the displacement response of damped and undamped piers is not different. The amplitude and duration of the displacement response of the rocking pier increase significantly when R=3, and the displacement response of the damped pier is slightly smaller than that of the undamped pier. By synthesizing the results of R=4 and R=5, it can be found that with the increase of mass ratio, the overall amplitude of the displacement response curve of the damped bridge pier gradually increases, and even exceeds that of the undamped bridge pier. This phenomenon can be clearly reflected when R=5, that is, after experiencing the peak displacement, the displacement response of the damped bridge pier exceeds that of the undamped bridge pier in 5s to 17s.

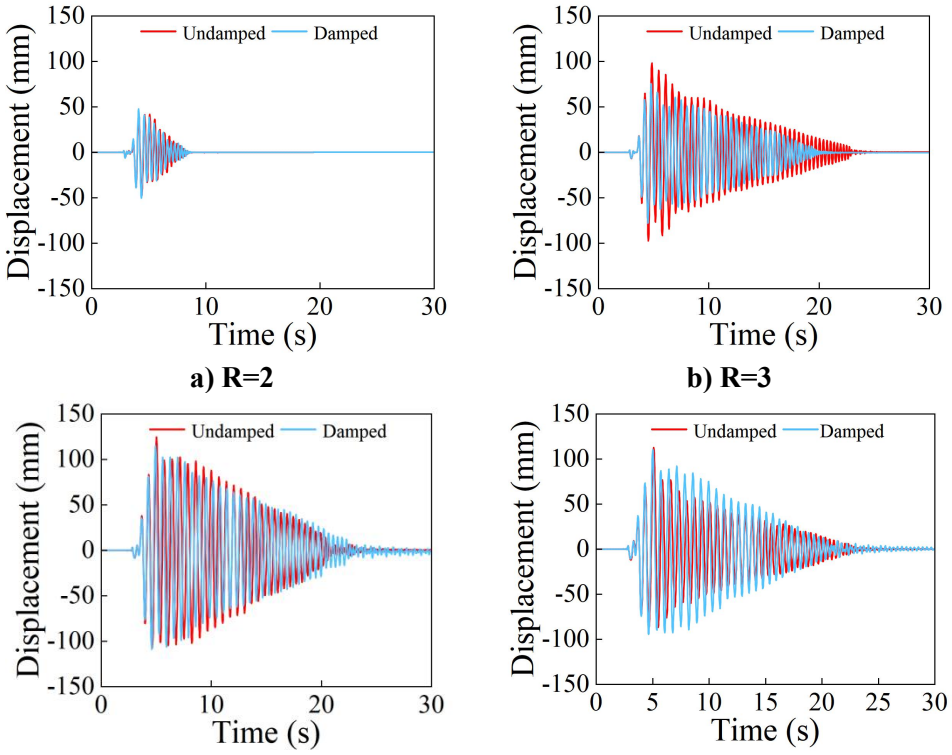

Figure 4. Displacement Response under Near-Field Impulse Earthquake with Different Mass Ratios

The displacement responses of different mass ratios under near-field non-impulse earthquakes are shown in Figure 5. It can be observed that when the mass ratio R=2, the displacement response of the undamped pier occurs larger, while the displacement response of the damped

pier is small. After the mass ratio gradually increases, it can be found that the displacement response of the damped pier is greater than that of the undamped pier. And with the increase of the mass ratio, the displacement response amplitude of the pier increases and the duration also becomes longer.

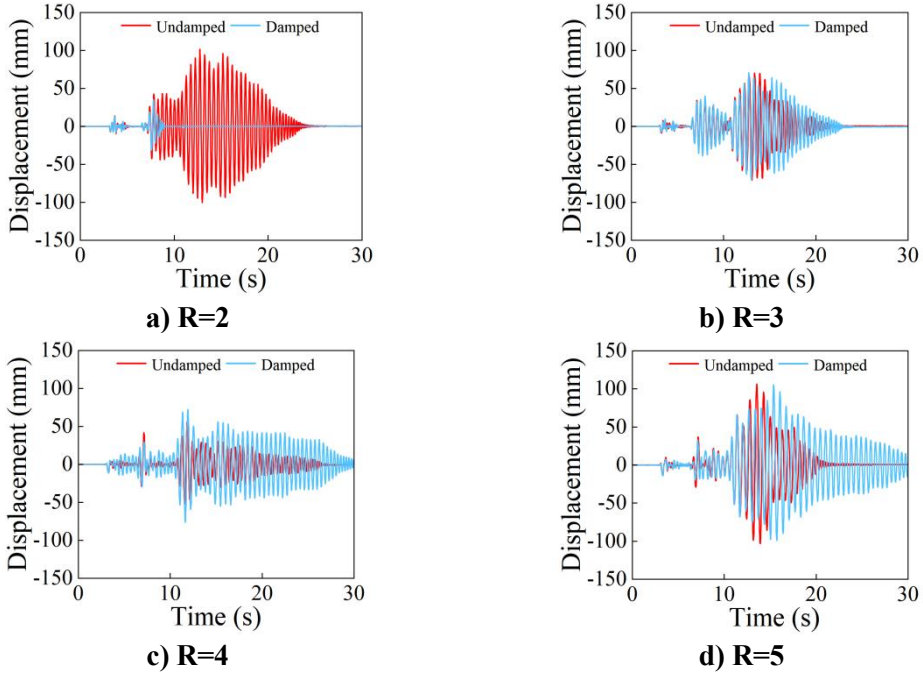

a) R=2 b) R=3

c) R=4 d) R=5

Figure 5. Displacement Responses with Different Mass Ratios under Near-Field Non-Impulse Earthquakes

For the displacement response results of different mass ratios under far-field earthquakes, as shown in Figure 6, the overall displacement response is still smaller than that under near-field earthquakes. At the same time, it can be seen that with the increase of mass ratio R, the overall displacement response has the largest amplitude and the longest duration when R=5. And except for R=2, the displacement response of damped piers at different times is greater than that of undamped piers.

2.2 Discussion of Question

For the above-mentioned large change in the displacement response of the bridge pier when R=3, the undamped bridge pier is taken as an example, and a more detailed analysis is carried out in the range of R=2 to R=3. The results are shown in Figure 7. It can be seen that with the increase of the mass ratio, the displacement response of the rocking bridge pier is gradually increased, and its duration does not continue to become longer when it reaches about 20s, which is related to the characteristics of ground motion. The reason why the small mass ratio R leads to the small dynamic response of the rocking bridge pier is that the lower mass of the superstructure leads to the lower inertial force, which is not enough to stimulate the swaying behavior of the bridge pier.

For the case where the displacement response of the damped rocking pier in the previous section is greater than that of the undamped rocking pier, this can be considered because the damping hinders the reset of the rocking pier to a certain extent. This situation is illustrated as shown in Figure 8. When the pier swings and tilts to the right, and the acceleration direction at the bottom of the pier is to the right, the pier will tend to reset in this case, but because the tension of the right damper will hinder the reset of the pier to some extent, the undamped pier may have a smaller corner, which can be reflected in Figure 8a. And then when the acceleration direction changes to the left, it will further cause the pier to tilt to the right, resulting in the continued increase of the pier angle, and due to the superposition of the above-mentioned corners in Figure 8a, it will lead to Figure 8b. The corner theta subscript 2 of the damped pier is larger than the corner theta subscript 1 of the undamped pier. After many such scenarios occur, the displacement response of the damped pier will be greater than that of the undamped pier.

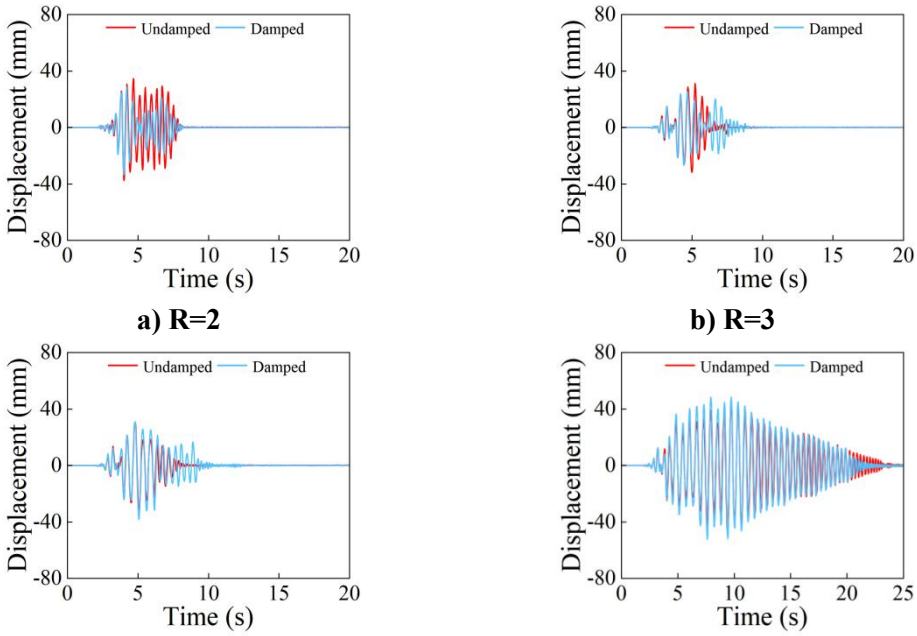

a) R=2 b) R=3

c) R=4 d) R=5

Figure 6. Displacement Responses of Different Mass Ratios under Far-Field Earthquakes

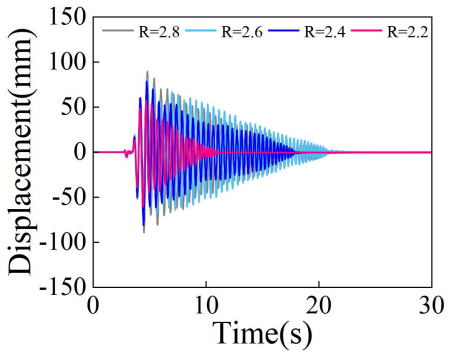

Figure 7. Displacement Response of Rocking Piers under Different Mass Ratios

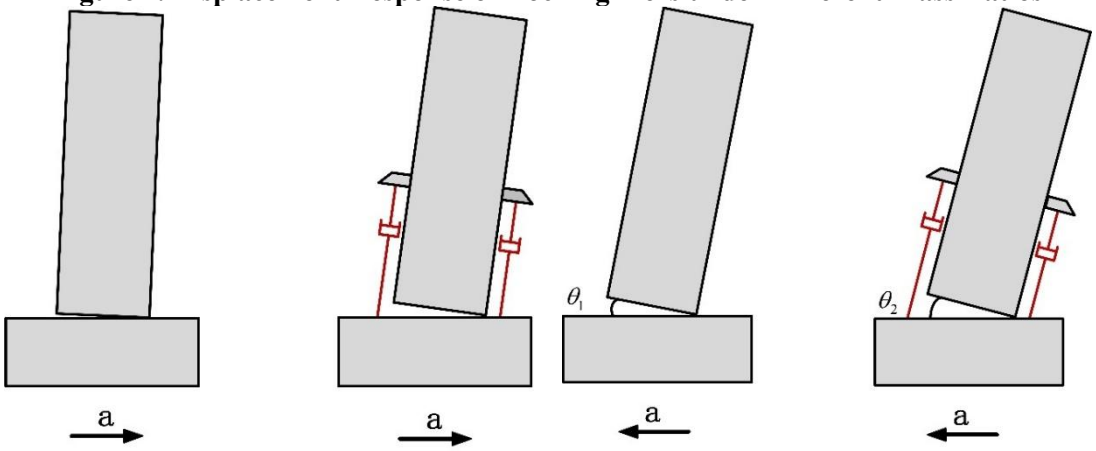

a)Acceleration to the left **b) Acceleration to the right**

Figure 8. Diagram of Rocking Pier Reset

3. Conclusion

In order to explore the influence of the ratio of the mass of the superstructure to the mass of the bridge pier on the seismic response of the rocking pier, this paper simulates the dynamic response of the rocking pier with different mass ratios under homologous earthquake action, and compares and analyzes the damped pier and the undamped pier. The conclusions are as follows:

Under normal circumstances, as the mass ratio increases, the dynamic response of the bridge pier will also increase, because the mass of the superstructure is positively correlated with the inertia force. At the same time, when the mass of the superstructure is small, due to the small inertia force, it is difficult to stimulate the pier to swing.

The displacement response of the rocking piers with small damping is larger than that of the rocking piers without damping, which is mainly due to the fact that the damping will hinder the resetting of the piers in the rocking behavior to a certain extent, resulting in the superposition of pier corners, which in turn causes this phenomenon.

References

[1] Binici B. Design of FRPs in circular bridge column retrofits for ductility enhancement [J]. Engineering Structures, 2008, 30(3): 766-776.

[2] Cheon J H, Lee J H, Kim T H, et al. Inelastic behaviour and ductility capacity of circular hollow reinforced concrete bridge columns under earthquake [J]. Magazine of Concrete Research, 2012, 64(10): 919-930.

[3] Beck J L, Skinner R I. The seismic response of a reinforced concrete bridge column designed to step [J]. Earthquake Engineering and Structural Dynamics, 1973, 2(4): 343-358.

[4] Zahn F A, Park R, Priestley M J N. Design of reinforced concrete bridge columns for strength and ductility [J]. Research Report, University of Canterbury, Christchurch, New Zealand, 1986, 86(7).

[5] Priestley M J N, Park R. Strength and ductility of concrete bridge columns under seismic loading [J]. Aci Structural Journal, 1987, 84(1): 61-76.

[6] Mamaghani I H P. Seismic Design and Ductility Evaluation of Thin-Walled Steel Bridge Columns of Box Sections [J]. Transportation Research Record, 2008, (2050): 137-142.

[7] F. L C. Discussion on Bridge Damage in Wenchuan Earthquake and Seismic Ductility Design [J]. Journal of Highway and Transportation Research and Development, 2009, 26(4).

[8] Bruneau M, Chang S E, Eguchi R T, et al. A framework to quantitatively assess and enhance the seismic resilience of communities [J]. Earthquake Spectra, 2003, 19(4): 733-752.

[9] Lv Xilin, Quan Liumeng, Jiang Huanjun. Research Trend of Earthquake Resilient Structures Seenfrom 16WCEE [J]. Earthquake Engineering and Engineering Dynamics, 2017, 37(3): 1-9.

[10] Du Xiuli, Zhou Yulong, Han Qiang, et al. State-of-the-art on rocking piers [J]. Earthquake Engineering and Engineering Dynamics, 2018, 38 (05): 1-11.

[11] Han Qiang, Jia Zhenlei, Zhou Yulong, e t al. Review of Seismic Resilient Bridge Str ucture: Rocking Bridiges [J]. Chinese Journal of Highways, 2021, 34 (02): 118-133.

[12] Mander J B, Cheng C-T. Seismic resistance of bridge columns based on damage avoidance design [M]. Seismic resistance of bridge columns based on damage avoidance design. 1997: 109.

[13] Cheng C T. Shaking Tab. tests of a self-centering designed bridge substructure [J]. Engineering Structures, 2008, 30(12): 3426-3433.

[14] Han Q, Jia Z L, Xu K, et al. Hysteretic behavior investigation of self-centering double-column rocking columns for seismic resilience [J]. Engineering Structures, 2019, 188: 218-232.

[15] Guo T, Cao Z L, Xu Z K, et al. Cyclic Load Tests on Self-Centering Concrete Column with External Dissipators and Enhanced Durability [J]. Journal of Structural Engineering, 2016, 142(1).

[16] Antonellis G, Panagiotou M. Seismic Response of Bridges with Rocking Foundations Compared to Fixed-Base Bridges at a Near-Fault Site [J]. Journal of Bridge Engineering, 2014, 19(5).

[17] Demir A, Caglar N, Ozturk H, et al. Nonlinear finite element study on the improvement of shear capacity in reinforced concrete T-Section beams by an alternative diagonal shear reinforcement [J]. Engineering Structures, 2016, 120: 158-165.

[18] Zhu H Q, Stephens M T, Roeder C W, et al. Inelastic response prediction of CFST columns and connections subjected to lateral loading [J]. Journal of Constructional Steel Research, 2017, 132: 130-140.

[19] Yang D X, Guo G Q, Liu Y H, et al. Dimensional response analysis of bilinear SDOF systems under near-fault ground motions with intrinsic length scale [J]. Soil

Dynamics and Earthquake Engineering, 2019, 116: 397-408.
[20] Alonso-Rodríguez A, Miranda E. Assessment of building behavior under near-fault pulse-like ground motions through simplified models [J]. Soil Dynamics and Earthquake Engineering, 2015, 79: 47-58.
[21] Dabaghi M, Der Kiureghian A. Stochastic model for simulation of near-fault ground motions [J]. Earthquake Engineering & Structural Dynamics, 2017, 46(6): 963-984.
[22] Moustafa A, Takewaki I. Deterministic and probabilistic representation of near-field pulse-like ground motion [J]. Soil Dynamics and Earthquake Engineering, 2010, 30(5): 412-422.

